Internat. J. Math. & Math. Sci.
VOL. 15 NO. 3 (1992) 563-580

COMPUTER TWO DIMENSIONAL MAPS OF LOOP SOLITON LATTICE SYSTEMS USING THE NEW APPROACH TO THE NO INTEGRABILITY AESTHETIC FIELD EQUATIONS

M. MURASKIN

University of North Dakota
Physics Department
Grand Forks, ND 58201

(Received May 9, 1991 and in revised form December 21, 1991)

ABSTRACT. We show that there are varieties of somewhat different loop soliton lattices when we specify an integration path in No Integrability Aesthetic Field Theory. These are illustrated using two dimensional computer maps. We have previously studied several such systems using the new approach to non-integrable systems developed in previous papers. [1-3]. The results of these earlier papers indicated that the solitons were rearranged by the new integration scheme in an erratic looking manner. However, we were restricted to regions close to the origin in these studies. With additional computer time made available and the use of tapes to store large amounts of information we have studied the above loop soliton systems and have been able to map considerable larger regions of the x,y plane. Symmetries for locations of the planar maxima and minima have been uncovered within a particular quadrant, although the symmetry found is not as great as the lattice. The type symmetry found is not maintained when more than one quadrant is involved. We also study a system that can be looked at as a perturbation of a loop lattice system. A brief discussion of the background material appears in the appendix.

1. INTRODUCTION.

We have proposed a new integration scheme to handle non-integrable equations [1-3] and have applied this method to the Aesthetic Field Equations [4-6]. In this approach there is but a single change function at each point. The role of the field equations is to determine change between a point and its neighbors (neighboring points lie on lines parallel to the coordinate axes). From data at a single point we can in this approach calculate the field throughout three dimensional space. Then, this information enables us to calculate the field on succeeding hypersurfaces. It is not necessary to make us of past history in such a calculation.

We have argued that non-integrable systems can be considered more natural than integrable systems as one can look at integrability as unduly restrictive [4]. Also, different integration paths traverse different environments, so it can be considered unnatural to expect that different integration paths give identical results.

We shall, in this paper, consider soliton solutions to the Aesthetic Field Equations [4]. We have obtained the following solutions when we specify an integration path:

1) Point lattice soliton systems in three dimensional space-time (soliton solutions are characterized in our work by the magnitude of the maxima (minima) not changing in time).

2) Closed string (loop) lattice solitons in four dimensional space-time.

The questions arise of how the additional degree of freedom associated with the new integration scheme affects the soliton solutions. The additional degree of freedom takes the form of a linear superposition principle at each point. The superposition principle collapses into a single contribution when the integrability equations are satisfied.

We have previously [1-3] studied the two types of soliton systems above using the new integration scheme. However, we were constrained to regions close to the origin due to limitations in computer time and to numerical errors distorting the results. Nevertheless, we were able to draw some definite conclusions even with coarse grids.

For the point soliton system we found that solitons could not be followed in time for as long as we wish due to solitons appearing and disappearing.

For the loop soliton systems we found that not all solitons have similar structure. We found evidence for a loop structure. We also found evidence for string solutions which did not close in the region studied. In one instance the computer run took one hundred hours of CPU time on the North Dakota IBM 3090.

We found that the soliton magnitude obtained when we specified an integration path was preserved by the new integration scheme.

Additional computer time has been made available enabling us to study considerably larger regions of space in this paper. The work here has been made possible by storing large amounts of information on tapes. The present more detailed investigation is restricted to $z = 0$, $x^0 = 0$ maps as a three dimensional detailed calculation still involves more computer time than we presently have available.

The soliton property enables us to have a handle on the error problem. Deviations from the soliton magnitude implies errors are a factor. In this case we can redo the calculation with a smaller grid size if the errors are greater than an allowed tolerance.

In this paper we have made use of the grid size .00234375 which is a factor 12 smaller than our most coarse grids used in References 2 and 3 where we already were able to draw definite results when we stayed close to the origin.

In the study we find several types of loop lattice, when we specify a path within the Aesthetic Field Theory, having different properties.

II. Point Soliton Lattice System

We continue our study of the data in Reference 2. Here, Γ^i_{jk} is taken to be

1) $\Gamma^1_{32} = 1.0 \quad \Gamma^3_{12} = -1.0$

$\Gamma^2_{31} = -1.0 \quad \Gamma^3_{21} = 1.0$

with the other $\Gamma^i_{jk} = 0$.

To get away from such simple values we integrate along x, then y, then z, then y, then x and then z going 700 points for each segment with grid size .003. The resulting Γ^i_{jk} we then used as origin point data. This system is intrinsically of a three space-time dimensional character. The z axis is referred to as the time axis.

This system was studied previously in Reference 2. Note Figure 8 of this reference which occurs when we specify an integration path and Figure 9 of this reference which results when we apply the new approach to no integrability. The component mapped is Γ^1_{33}. We see that Figure 9 suggests a more disorderly system than the lattice of Figure 8 although we do see the following symmetry: When $x \rightarrow -x$ and positive number go into negative numbers we see a similar system of

contour lines (except in the immediate region close to $x = 0$).

Within any particular quadrant no obvious symmetry was apparent.

An important result obtained in Reference 2 was that the soliton magnitude .49 was maintained by the integration scheme. The solitons could then be said to be rearranged from the lattice position. Evidence is also presented in Reference 2 that trajectories of solitons cannot be followed in time for as long as we wish due to solitons appearing and disappearing. This has led us to remark nonintegrable systems may ultimately account for quantum type behavior. This emphasizes that an understanding of exactly what sorts of effects can be attributed to the new integration scheme, when applied to a lattice system, would be of value.

We may ask---does the rearrangement of the solitons by the new integration scheme lead to what resembles an erratic distribution of solitons? Or does a mapping of a large region of space reveal a symmetric pattern for the solitons?

The results of our present study of the system associated with (1) is given in Figure 1. The $+\ -$ quadrant is mapped with .00234375 grid. We mapped 8,076 points along x and 2,687 along y. We note maxima (minima) having values of $\pm$ .49 and $\pm$ .23. No deviations from these maxima (minima) numbers was obtained in the region mapped indicating that numerical errors are not a problem for the grid size used. We find that the location of maxima (minima) do not at all simulate a random system. Thus, it is easy to be deceived by the small region mapped in Reference 2.

Consider any maxima (minima) in the $+\ -$ quadrant. If we proceed 40 units in x and then 40 units in $-y$ (each units 48 $\times$.00234375), we then coma across a maximum (minimum) of the same magnitude.

In the 45 degrees diagonal direction we come across four different structures (as indicated by the contour lines in Figure 1) then our results suggest that this structure repeats.

If we look at a maximum (minimum) in, say, the $-\ -$ quadrant and then go over forty units in $-y$ and forty units in x thereby entering the $+\ -$ quadrant we do not find any maximum (minimum). Thus, the symmetry is not respected when more than one quadrant is involved.

Maxima and minima to the right of the $x = -y$ line are located in a regular way as we increase x. For example, we have a maximum of .237 at $x = 17$, $y = -4\,\frac{1}{2}$. This maximum is repeated at $x = 73$, $y = -4$ and $x = 128$, $y = -4$. Thus, we see a repeat of the maxima when $\Delta x = 56 \pm 1$. The results of Section V suggest that we have a repeat of maxima (minima) as a function of y for maxima (minima) to the left of the $x = -y$ line. However, Figure 1 is not deep enough in y to confirm this here.

Consider the maximum .237 at $x = 17$, $y = -4\,\frac{1}{2}$. We proceed along the 45 degree direction (as measured downward from the $+x$ axis). We then cut along contour lines as shown by Figure 1. If we go to the right 56 units in x to another similar maximum and then proceed along the 45 degree line the contour lines that are cut have a different character. The location of successive maxima (minima) to the right of the $x = -y$ line can be predicted according to a pattern -- but the contour lines in the vicinity of a particular maximum (minimum) can be different than the contour lines around another maximum (minimum). An example of this effect is the minimum $-.498$ at $x = 19$, $y = -10$. If we go to $x = 75$, $y = -10$ we see another minimum of magnitude $-.498$. However, the $-.400$ contour lines surrounding the two minima are not similar.

The conclusion we reach in this Section is that the new approach to no integrability leads to a marked symmetry pattern within a quadrant. However, the symmetry is not as great as the

lattice. We have different structures on one side of the $x = -y$ line as compared to the other side. Contour lines surrounding the maxima can depend on its location. Also we have what can be called a quadrant effect. The symmetric pattern of repeating maxima (minima) after proceeding forty units in x and minus forty units in y is not valid when proceeding across a coordinate axis.

III. A Loop Lattice Soliton System

We now use data (1) in conjunction with a four dimensional e_i^α given in Equation (3). This data is the same as used in Reference 1. We also later studied this system in reference 7 and 8.

When we specify an integration path we obtain a map given by Figure 2 of Reference 7. The map is for Γ^1_{11}. In three spatial dimensions we see a loop lattice (Figures 1 and 2 of Reference 8).

This data differs from that of Section II in that it describes a four dimensional space-time system.

In Reference 1 we studied this system using the new integration scheme (note Figure 2 there). The region studied was not large enough to uncover symmetries within a quadrant. Thus, Figure 2 of Reference 1 might well suggest something of an erratic pattern for the soliton maxima (minima) of magnitude .64.

The soliton magnitude of .64 was also present when we specify an integration path.

We did not observe the symmetry between quadrants when $x \to -x$ and positive numbers go into negative numbers as we observed in Section II. However, we note that maxima having the value of .64 occurred only in the $+\,-$ and $-\,+$ quadrants and minima of magnitude .64 only occurred in the $+\,+$ and $-\,-$ quadrants.

Other magnitudes besides .64 occurred for maxima (minima) within the map.

This system was again studied with the finer grid used in Section II and over a larger region of space. The results are given in Figure 2 for $+\,-$ quadrant. The map is for Γ^1_{11}. The larger region enables us to unmask a symmetric pattern reminiscent of Figure 1. Starting with a planar maximum (minimum) we then proceed 36 units in x and 36 units in $-y$. We then come across another planar maximum (minimum) of the same magnitude.

This data was slightly more sensitive to error than the data of Figure 1 as $\pm$ .64 appears as $\pm$ .62 farther from the origin.

The contour lines had a different shape in Figure 2 as compared with Figure 1, but otherwise the symmetry pattern uncovered within a quadrant resembled one another in the two instances. The next question is whether there exists other soliton loop lattices of different character (as compared with Figure 2 of Reference 7). Do other such soliton loop lattices have similar symmetries as seen in this section when we apply the new integration scheme?

IV. A Third Set of Data

Consider the following $\Gamma^\alpha_{\beta\gamma}$

(2) $\Gamma^1_{32} = \Gamma^2_{13} = \Gamma^3_{21} = -\Gamma^1_{23} = -\Gamma^2_{31} = -\Gamma^3_{12} = 1.0$

$\Gamma^1_{02} = -\Gamma^2_{01} = 1.0$

$\Gamma^1_{03} = -\Gamma^3_{01} = .8$

$\Gamma^2_{03} = -\Gamma^3_{02} = .6$

Γ^i_{jk} is then obtained using the following e^α_i

$$(3)\quad e^\alpha_i = \begin{pmatrix} .88 & -.42 & -.32 & .22 \\ .5 & .9 & -.425 & .3 \\ .2 & -.55 & .89 & .6 \\ .44 & -.16 & .39 & 1.01 \end{pmatrix}$$

Use is made of

$$(4)\quad \Gamma^i_{jk} = e_\alpha{}^i e^\beta_j e^\gamma_k \Gamma^\alpha_{\beta\gamma}$$

This data was not studied previously. When we specify a path by first integrating x^0, then z, then y and then x, we get the map of Figure 3 when $z = -1.5$. Three dimensional studies again indicate a loop soliton lattice with maxima (minima) having the magnitude of .95.

Comparing Figure 3 with Figure 2 of Reference 7 we note the following: The closed contour lines of Reference 7 point to the right and then to the left as we varied y. The pattern is repeated. On the other hand, the closed loops of Figure 3 all point towards the right. Thus, this loop lattice has a somewhat different character.

The results applying the new integration scheme is given in Figure 4.

In Figure 4 we study the $+\ -$ quadrant for Γ^1_{11}. We find planar minima having the soliton magnitude of .95. The $+\ -$ quadrant has regions of positive numbers surrounded by a sea of negative numbers with maxima having magnitude of .77. There is also a maxima of magnitude of .30 close to the $x = 0$ axis.

The basic symmetry which appeared in the previous sections is present here as well. Proceeding from a maximum (minimum) 24 units in the x direction and 24 units in the $-y$ direction leads to a similar maximum (minimum). This type of symmetry we shall see is present for all the loop soliton lattices that we have studied.

In the $-\ -$ quadrant the contour lines are different looking. Here outside the region close to $x = 0$ we see planar minima of magnitude .82. In this case the negative numbers are surrounded by a sea of positive numbers. The maxima have magnitude .95 which is the soliton magnitude.

In the $+\ -$ quadrant we note different types of structures to the left of the $x = -y$ line as compared to the right of this line. This effect is pronounced here although it is also present for the other soliton loop lattices we study (including the system of Section III although it was not as pronounced in Figure 2).

V. A Fourth Set of Data

Consider the following Γ^i_{jk}

$$(5)\quad \Gamma^1_{23} = \Gamma^2_{31} = \Gamma^3_{12} = -\Gamma^1_{32} = -\Gamma^2_{13} = -\Gamma^3_{21} = 1.0$$

$$\Gamma^1_{20} = \Gamma^1_{02} = \Gamma^0_{21} = -\Gamma^0_{12} = -\Gamma^2_{10} = -\Gamma^2_{01} = 1.0$$

$$\Gamma^3_{10} = \Gamma^3_{01} = \Gamma^0_{13} = -\Gamma^0_{31} = -\Gamma^1_{30} = -\Gamma^1_{03} = 1.0$$

$$\Gamma^2_{30} = \Gamma^2_{03} = \Gamma^0_{32} = -\Gamma^0_{23} = -\Gamma^3_{20} = -\Gamma^3_{02} = 1.0$$

the other Γ^i_{jk} are zero. This set of data has not been studied previously.

We specify a path in the manner discussed previously and map Γ^1_{00}. The result is given in Figure 5. This set of data leads to a soliton loop lattice but with two types of maxima (minima) having the magnitudes 1.36 and .50. In our previous sets of data there was but one magnitude for the maxima (minima) when we specify a path. We refer to the lattice of Figure 5 as a $\pm A$, $\pm B$ type lattice.

In Figure 5 we show $\pm .10$ contour lines.

In Figure 6 we apply the new integration scheme to this data. In this case we have studied the $+\ -$ quadrant with a greater depth in y.

The results indicated that we have the same magnitude for the maxima (minima) as when we specify a path, namely 1.36 and .50, although the data is more sensitive to error (the deviations from these numbers are as much as .06).

We note that within the $+\ -$ quadrant we have maxima and minima of magnitude 1.36. This feature was not present for the previous systems. In addition, within the $+\ -$ quadrant we also see maxima and minima of magnitude .50.

There is no obvious symmetry between the different quadrants.

Starting with a maximum (minimum) and going 20 units in x and 20 units in $-y$ we arrive at another maximum (minimum) of the same type as long as we stay in the same quadrant. Thus, the basic symmetry which we have seen previously is present for this more complicated system.

To the right of the $x = -y$ line we see maxima (minima) repeated with regular spacing as we vary x, while to the left of the $x = -y$ line we see maxima (minima) repeated with regular spacings as we vary y. This effect was suspected in Section II but we did not have enough depth in y to confirm the effect there.

Consider the minimum of magnitude 1.33 at $x = 24$, $y = -21$. This is slightly to the right of the $x = -y$ line. This minimum is repeated as we proceed 33 units in x with y unchanged. However, the .10 contour line slightly to the right of the maximum has a different character as we displace x. Thus, the symmetry in x is for the location of planar maxima (minima) and not for the contour lines in the vicinity. This feature is present as well for the different soliton loop lattices.

We find planar maxima (minima) other than the 1.36 and .50 magnitudes, but in the $-\ -$ and $+\ +$ quadrants. For example, a planar maxima of magnitude .33 shows up using a .0046875 grid close to $x = 0$ in the $-\ -$ quadrant and is repeated as we alter y.

VI. A Fifth Set of Data

Consider the following $\Gamma^\alpha_{\beta\gamma}$

(6) $\Gamma^1_{23} = \Gamma^1_{32} = \Gamma^3_{21} = -\Gamma^3_{12} = -\Gamma^2_{13} = -\Gamma^2_{31} = 1.0$

$$\Gamma^1_{20} = \Gamma^2_{01} = \Gamma^0_{21} = -\Gamma^1_{02} = -\Gamma^2_{10} = -\Gamma^0_{12} = .5$$

We then use the e^α_i given in (3) to obtain our origin point data. This data was not considered in any previous work.

We specify a path as before and then map Γ^1_{11} in Figure 7. This system is another example of a $\pm A$, $\pm B$ soliton loop lattice with magnitudes of maxima (minima) having the values 1.50 and .86. This set differs from the set of Section V as the different magnitudes lie below one another and not alongwise as well as in Figure 5.

The results of the new integration scheme is presented in Figure 8. We still see the 1.50 and

.86 magnitudes for maxima (minima) along with other magnitudes as well. In the $+\ -$ quadrant there are maxima of magnitude 1.5 and .86 while in the $-\ -$ quadrant we see minima of this magnitude. The sensitivity to error is comparable to the previous section.

When we go 45 units from the maximum (minimum) in x and 45 in $-y$ we obtain another maximum (minimum) of the same type as long as we stay within a single quadrant. The symmetries within the quadrant are similar to what we have seen previously.

We do not see any apparent symmetry between the $+\ -$ and $-\ -$ quadrants.

VII. A Sixth Set of Data

Consider the following $\Gamma^{\alpha}_{\beta\gamma}$

(7) $\Gamma^1_{02} = \Gamma^2_{03} = \Gamma^3_{01} = 1.0$

$\Gamma^1_{03} = \Gamma^2_{01} = \Gamma^3_{02} = -1.0$

$\Gamma^0_{13} = \Gamma^0_{21} = \Gamma^0_{32} = 1.0$

$\Gamma^0_{12} = \Gamma^0_{23} = \Gamma^0_{31} = -1.0$

We obtain origin point data using (3). This set of data was studied previously in Reference 3. When we specify an integration path we obtain Figure 2 of Reference 3 and when we use the new approach to integrability we obtain Figure 3 of Reference 3 for the quantity Γ^1_{11}.

We restudy the situation of Figure 3 of Reference 3. The results are given for the $+\ -$ quadrant in Figure 9. We do not see a symmetry between quadrants, but within the $+\ -$ quadrant we see the same type of symmetry that we have seen common to the other sets of data in this paper. For example, starting with a maximum (minimum) and going 23 units in x and 23 units in $-y$ leads to a maximum (minimum) of the same magnitude.

VIII. A Seventh Set of Data

Consider the following $\Gamma^{\alpha}_{\beta\gamma}$

(8) $\Gamma^1_{21} = -.5 \qquad \Gamma^1_{22} = -.5 \qquad \Gamma^1_{23} = .25$

$\Gamma^1_{31} = .4 \qquad \Gamma^1_{32} = -.25 \qquad \Gamma^1_{33} = .5$

$\Gamma^2_{11} = .5 \qquad \Gamma^2_{12} = .5 \qquad \Gamma^2_{13} = -.25$

$\Gamma^2_{31} = .25 \qquad \Gamma^2_{32} = -.4 \qquad \Gamma^2_{33} = -.5$

$\Gamma^3_{11} = -.4 \qquad \Gamma^3_{12} = .25 \qquad \Gamma^3_{13} = -.5$

$\Gamma^3_{21} = -.25 \qquad \Gamma^3_{22} = .4 \qquad \Gamma^3_{23} = .5$

using e^{α}_i given by (3) we then obtain the origin point data.

A map of Γ^1_{11} for the $+\ +$ quadrant is given by Figure 10 when we specify an integration path in the same manner as before. We note that Figure 10 look very similar to Figure 2 of Reference 3. However, the magnitudes of maxima and minima are not all the same, but vary from .85 to .94,

when use is made of a .01875 grid with spacing between points of $16 \times .01875$. Further computer runs with different size grids also show this variation in magnitude. There is no obvious pattern for the magnitudes that we have uncovered. Computer runs in z and x^0 do not show a soliton system as the magnitudes change in z and x^0. In Figure 10 we see some deviation from a rigorous lattice (note a 40 contour line appearing over one of the -40 contour lines and other small deviations from regularities).

If we connect up the planar maxima (minima) as we vary z we obtain a network in a fairly regular pattern.

We can think of Figure 10 as a kind of perturbation of the lattice of Figure 2 of Reference 3. The questions is what happens to this system when we apply the new integration scheme. This is shown in Figure 11 for Γ^1_{11}. Qualitatively we see a somewhat regular pattern but quantitatively we do not see the $\Delta x = a$, $\Delta y = -a$ symmetry that we have seen throughout this paper. Also the magnitude of planar maxima and minima does not remain the same.

This set of data illustrates that we need not restrict ourselves to soliton lattices within the theory.

IX. Summary

The only soliton system we have thus far obtained in Aesthetic Field Theory in four dimensional space-time is the loop lattice (when we specify an integration path). We have, in this paper, obtained several different varieties of loop lattice and have taken the opportunity to study them here. In three dimensional space-time we have also obtained a point soliton lattice.

We have on previous occasions studied how the soliton systems are affected by the new integration scheme [1-3] which allows for a superposition principle at all points off the coordinate axes. However, our results were constrained to regions close to the origin. In Figure 3 of Reference 3 an x, y map uncovered more than 50 planar maximum and minimum close to the origin in a pattern that appeared rather erratic. In this paper we have had available considerably more computer time. Also, we have made extensive use of tapes to store a large amount of information. With these aids we have uncovered clear cut symmetry patterns within a particular quadrant. The symmetry was found for all soliton lattices studied. The symmetry is not as great as the lattice. As we mentioned above, closer to the origin the planar maxima and minima appear to be located in a more disorderly fashion.

We also note that the soliton magnitudes are preserved by the integration scheme. We also found other magnitudes appearing as well.

An aim of our studies is to see whether the new integration scheme can rearrange soliton lattice particles from a symmetric lattice configuration to a disorderly type system. The idea under consideration is whether the new integration scheme can transform a "classical" system into a "quantum" system. The evidence in this paper shows clear cut symmetry within a quadrant. However, the type of symmetry observed is not present when more than one quadrant is involved. Also, within a quadrant the situation does not appear regular close to the origin. Thus, it was easy to be deceived by maps involving limited regions as in our previous work. Three and four dimensional studies would be useful in obtaining a better understanding of the system. What becomes of the non-regular looking regions as we integrate in z and x^0? A study of non lattice multiparticle solutions which we initiated in Section VIII may also be useful in generating disorderly looking multiparticle solutions.

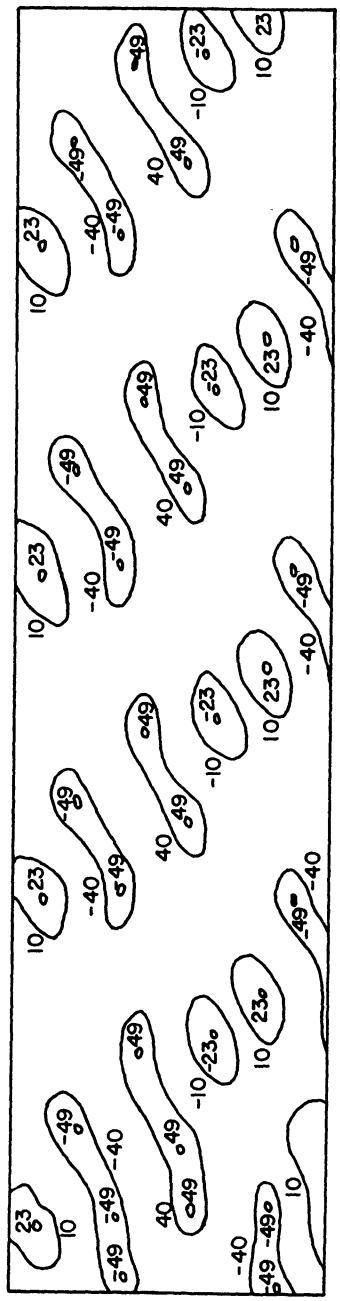

Figure 1 Three dimensional space-time data of Section II using the new integration scheme. Grid is .00234375. Map is for Γ^1_{33}. Numbers are 100 times actual numbers in this figure as well as the other figures. Map is for + − quadrant.

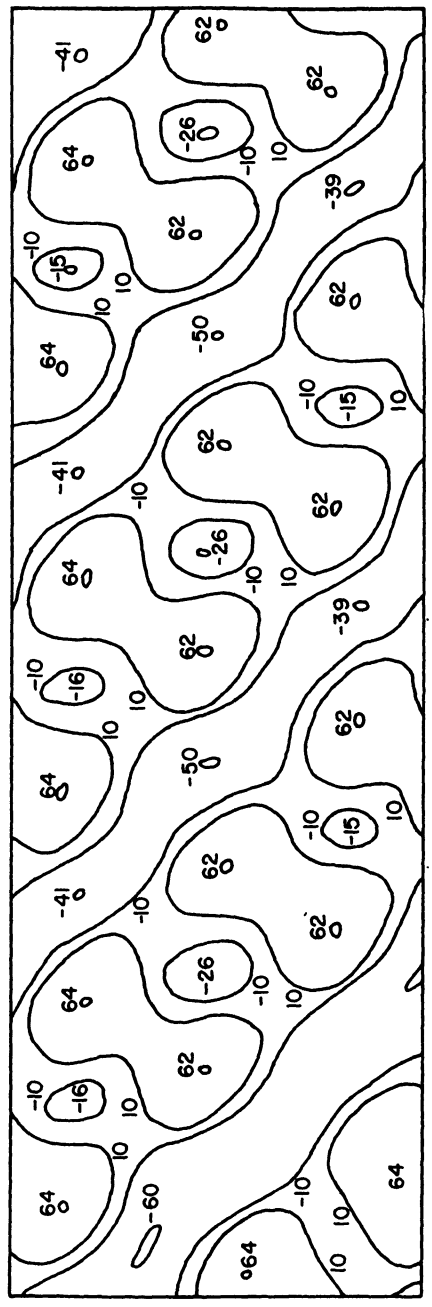

Figure 2 Data of Section III using the new integration scheme. Grid is .00234375. Map is for Γ^1_{11} in + − quadrant.

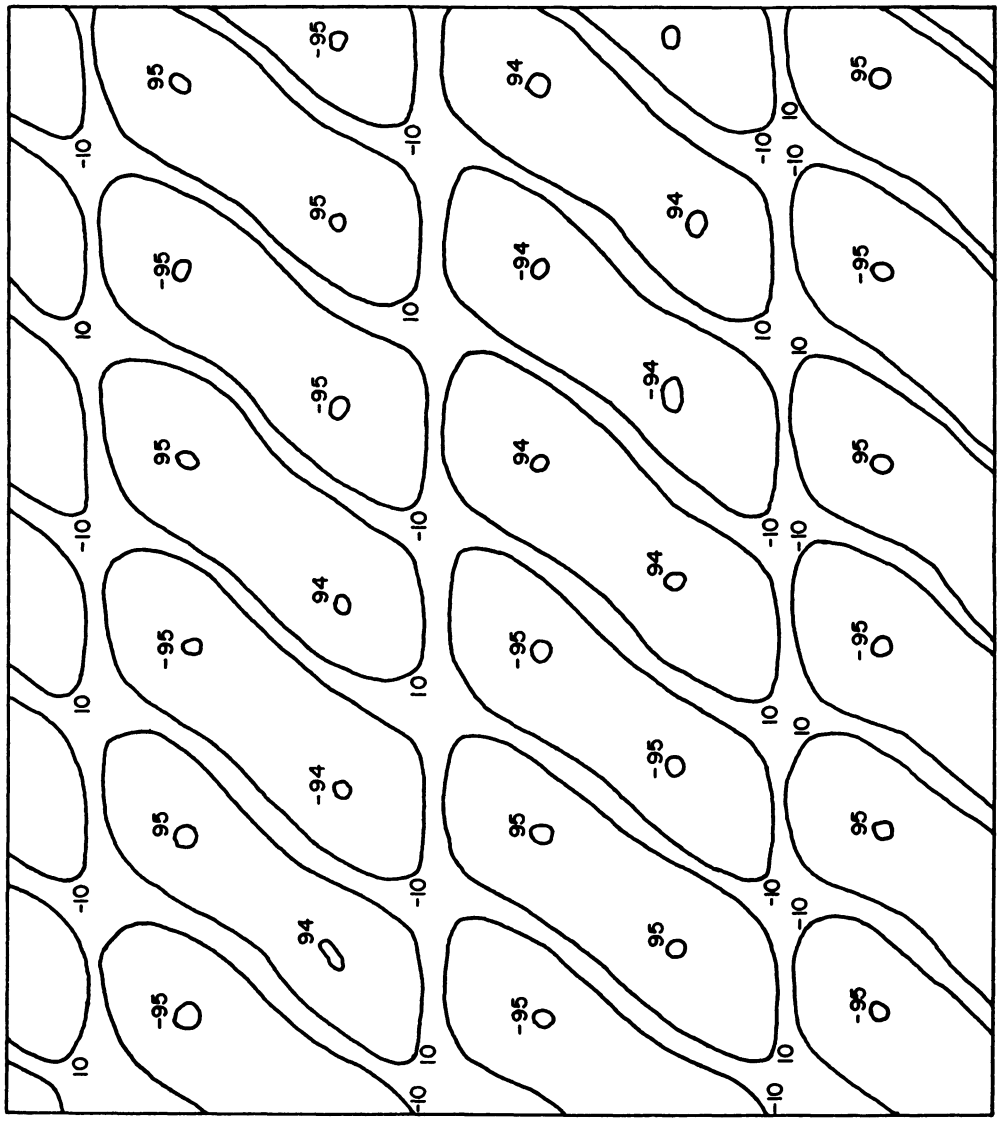

Figure 3 Data of Section IV specifying an integration path. Grid is .15. Map is for Γ^1_{11}.

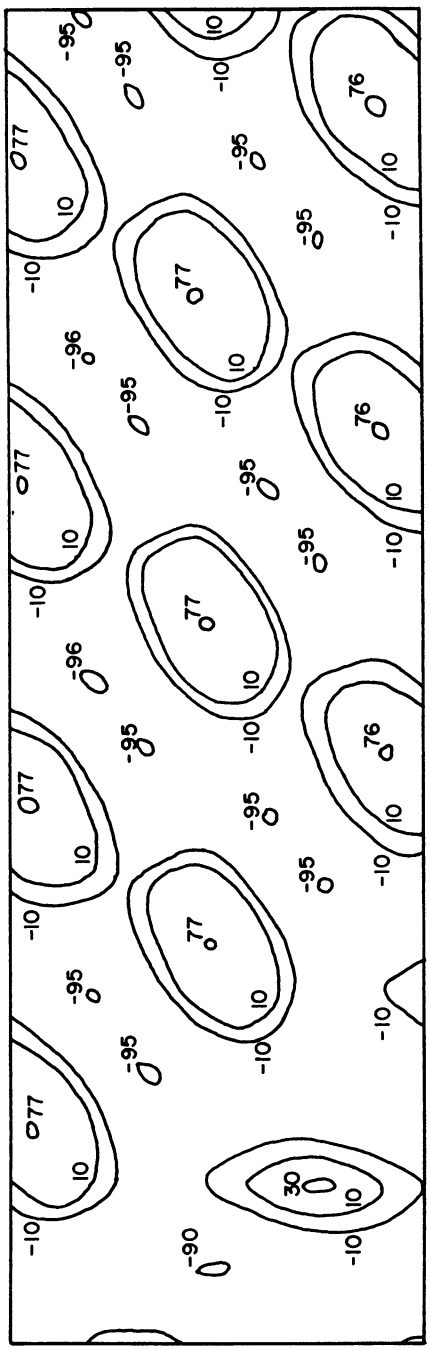

Figure 4 Data of Figure 3 using the new integration scheme. Grid is .00234375. Map is for Γ^1_{11} in + − quadrant.

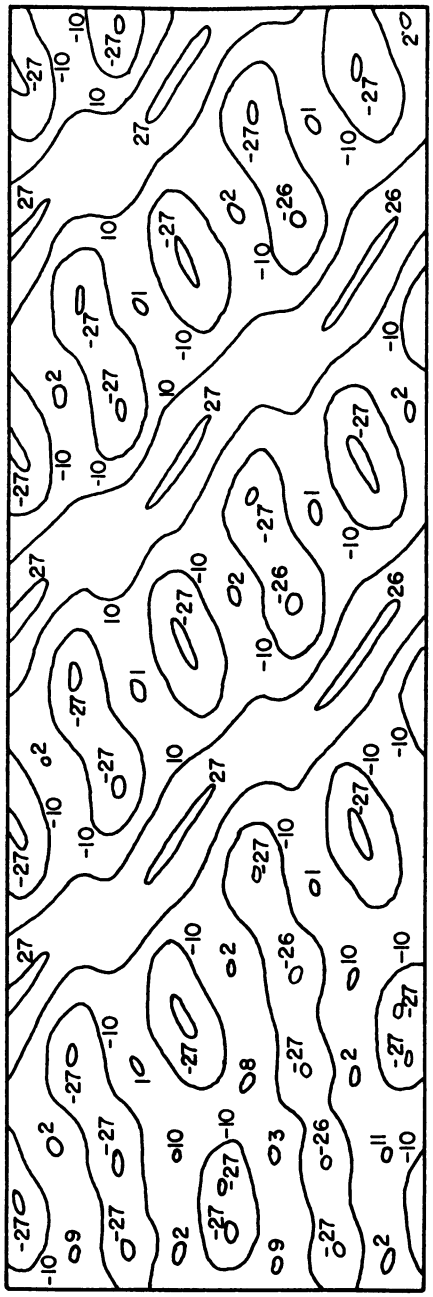

Figure 9 Data of Section VII using the new integration scheme. Grid is .00234375. Map is for Γ^1_{11} in + − quadrant.

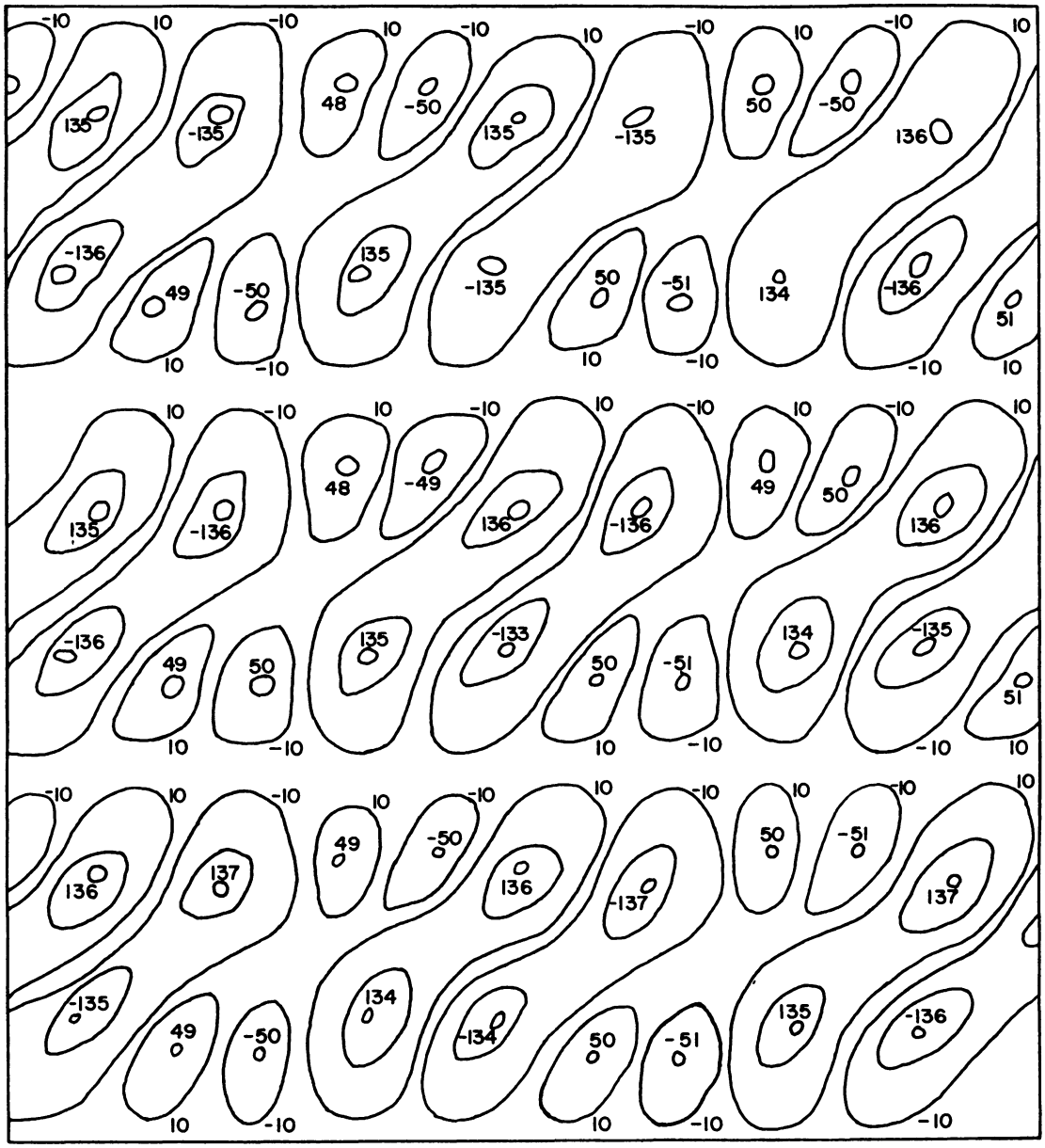

Figure 5 Data of Section V specifying an integration path. Grid is .075. Map is for Γ^1_{00}.

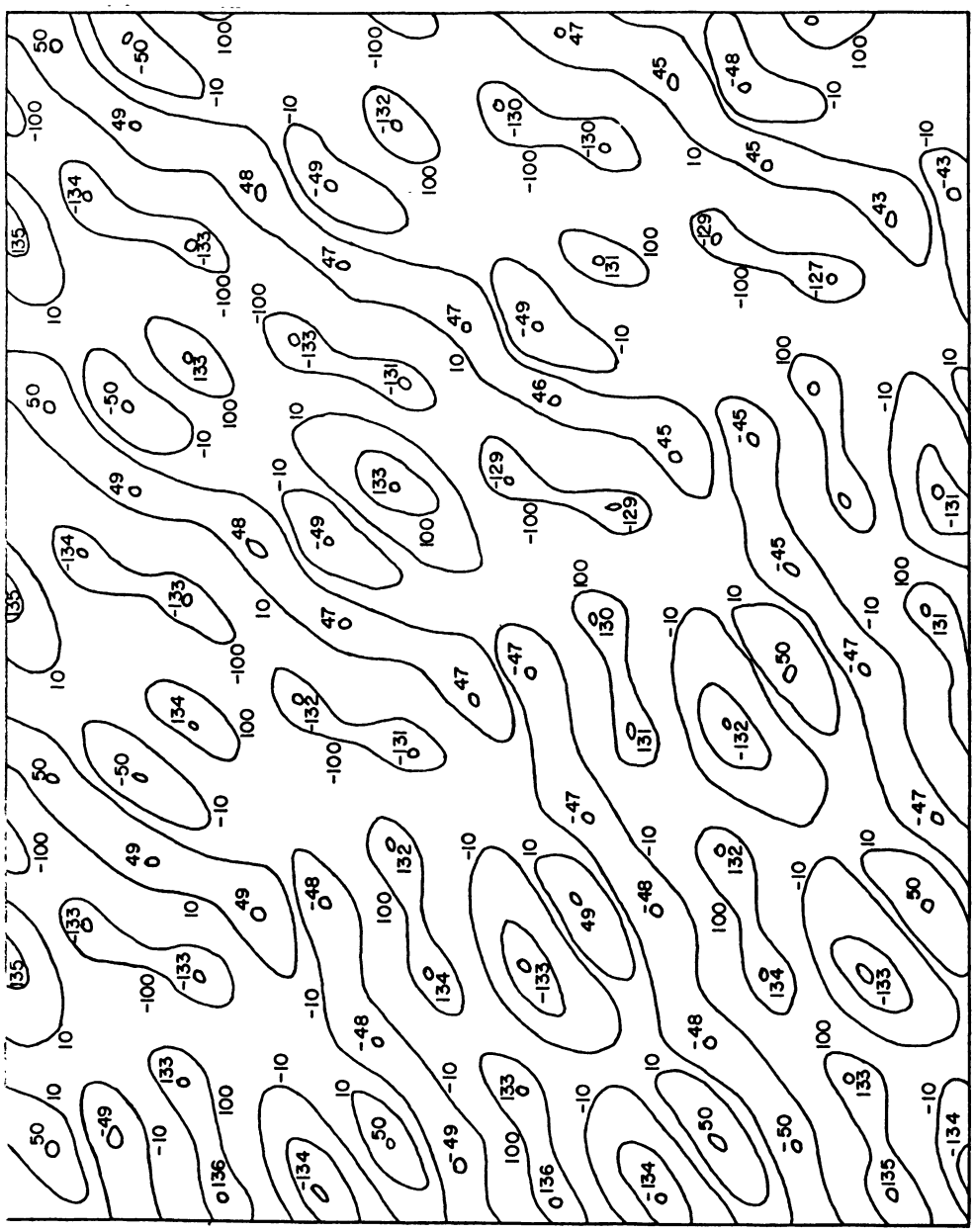

Figure 6 Data of Figure 5 using the new integration scheme. Grid is .00234375. Map is for Γ^1_{00} in + − quadrant.

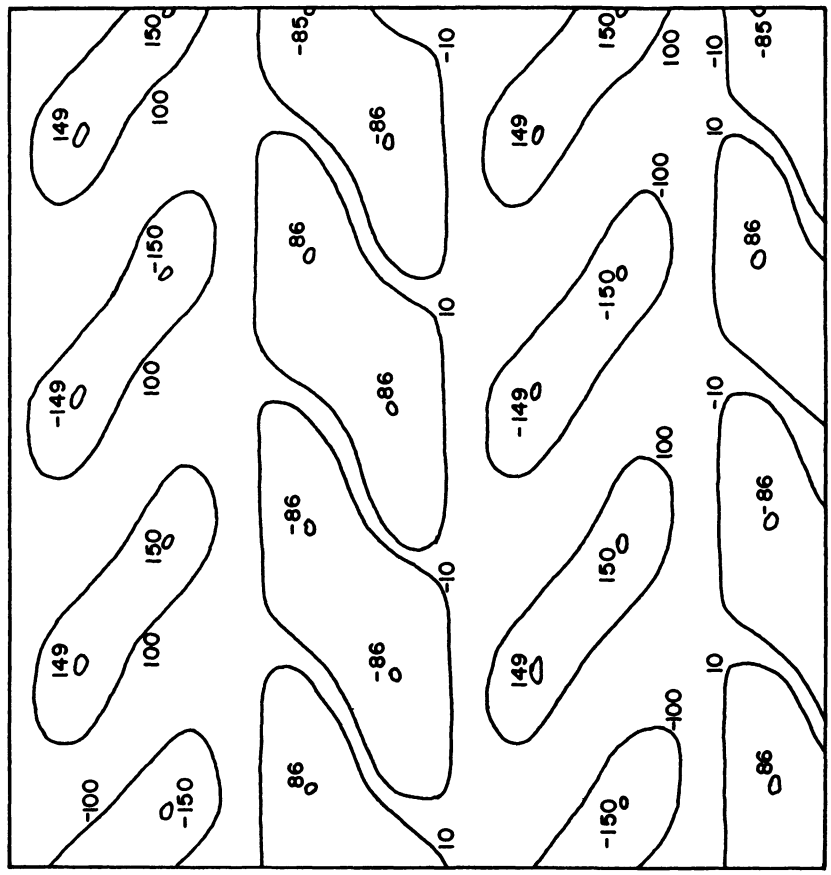

Figure 7 Data of Section VI specifying an integration path. Grid is .1. Map is for Γ^1_{11} in + − quadrant.

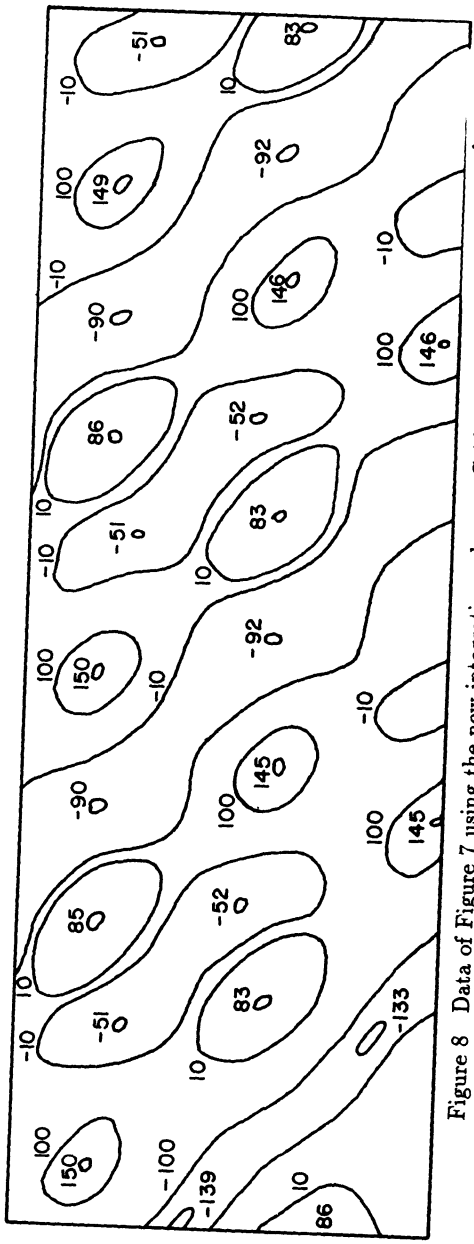

Figure 8 Data of Figure 7 using the new integration scheme. Grid is .00234375. Map is for Γ_{11}^1 in + − quadrant.

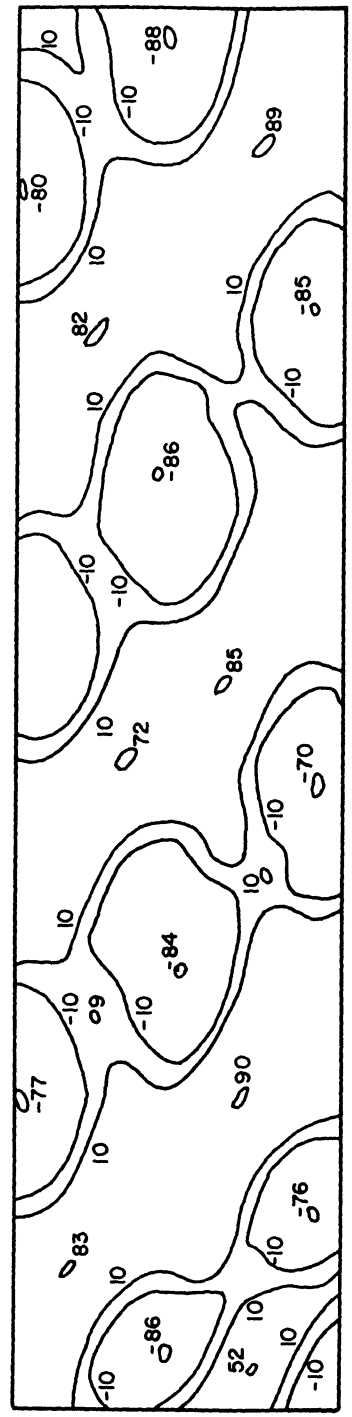

Figure 11 Data of Figure 10 using the new integration scheme. Grid is .00234375. Map is for Γ_{11}^1 is + − quadrant.

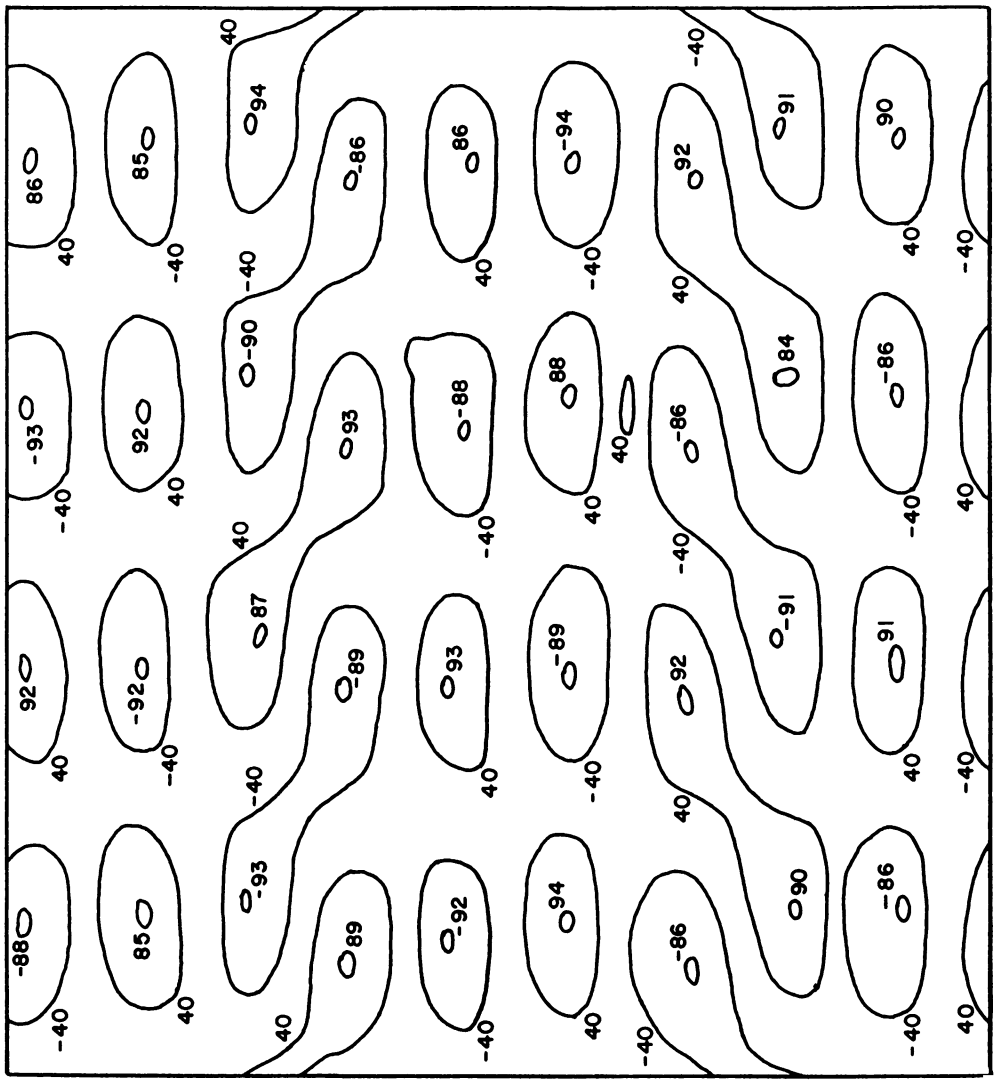

Figure 10 Data of Section VIII specifying an integration path. Map is for Γ^1_{11} using .01875 grid. The spacing between points is 16 × .01875.

APPENDIX

In the appendix we give some background for the material in the text.

The underlying hypothesis we make is that the foundations of physics lie in mathematical aesthetics (if not how can we ultimately justify one set of equations rather than another as there are fundamental limitations on empiricism). Another motivation, is that a system of mathematically aesthetic principles may have sufficient content that it may simulate the world of nature in some domain. Also, it may serve as a laboratory to study fundamental principles. As an example of this we cite our article "The Arrow of Time"[9]. The arrow of time is not tied to any specific set of field equations. We have found that this concept has a natural explanation within the aesthetic fields program.

In References 4 and 10 we have shown that there is such a concept as mathematically aesthetic principles; that these principles can be cast into the form of a set of nonlinear partial differential equations; and these equations have considerable content as evidenced by computer solutions.

Once one introduces the notion of Cartesian tensor one opens the door to tensors of all rank. We have, in our work, made the hypothesis that all Cartesian tensors, regardless of rank, should be treated in a uniform way with respect to change. This is the core of what we call Aesthetic Field Theory.

We also require that arbitrary data be supplied at a single point rather than on a hypersurface. This minimizes the arbitrariness of the theory. Also, if data were arbitrary on a hypersurface then particle structure, an aim of the theory, would also be arbitrary on the hypersurface.

As most theories admit a vector field we shall start off by assuming the existence of a vector A_i. We write for the change of A_i, between neighboring points

(A1) $$dA_i = \Gamma^j_{ik} A_j dx^k .$$

Γ^i_{jk} is a set of coefficients which we call the change function as it determines the change of A_i. We have dropped terms of higher order in dx^k. We allow for Γ^i_{jk} to be a function of A_i, among other things, to allow for greater generality. For a second vector field we write

(A2) $$dB_i = \Gamma^j_{ik} B_j dx^k .$$

Thus, we are assuming that Γ^i_{jk} is a universal change function that determines the change of all vectors in a uniform way. That is, one set of numbers corresponding to a vector should not be treated any differently from any other vector set of numbers. From the product $A_i B_j$ we have from (A1) and (A2)

(A3) $$d(A_i B_j) = (\Gamma^t_{ik} A_t B_j + \Gamma^t_{jk} A_i B_t) dx^k .$$

Now $A_i B_j$ is an example of a second rank tensor. We then require that Γ^i_{jk} determines the change of all second rank tensors in a uniform way. For a second rank tensor g_{ij} we then get

(A4) $$dg_{ij} = (\Gamma^t_{ik} g_{tj} + \Gamma^t_{jk} g_{it}) dx^k .$$

Going one step further, an nth rank tensor is taken to behave like a product of n vectors. From A_i, g_{ij}, we introduce A^i

(A5) $$A_i = g_{ij} A^j .$$

Then from (A1) and (A4), provided g_{ij} has an inverse, we get

(A6) $$dA^i = -\Gamma^i_{jk} A^j dx^k .$$

In a Cartesian system dA_i is a vector. Thus, Γ^i_{jk} is a third rank tensor from (A1) and thus behaves like $A^i B_j C_k$. Therefore, the change of Γ^i_{jk} is given by

(A7) $$d\Gamma^i_{jk} = (\Gamma^i_{mk}\, \Gamma^m_{jl} + \Gamma^i_{jm} \Gamma^m_{kl} - \Gamma^m_{jk}\, \Gamma^i_{ml}) dx^l .$$

Then from

(A8) $$d\Gamma^i_{jk} = \frac{\partial \Gamma^i_{jk}}{\partial x^l}\, dx^l ,$$

we get the "aesthetic field equations"

(A9) $$\frac{\partial \Gamma^i_{jk}}{\partial x^l} = \Gamma^i_{mk}\, \Gamma^m_{jl} + \Gamma^i_{jm}\, \Gamma^m_{kl} - \Gamma^m_{jk}\, \Gamma^i_{ml} .$$

These equations involve the change function alone. Γ^i_{jk} at all points is determined in terms of Γ^i_{jk} at a single point. We see from (A9) that derivatives of gamma are given by products of gamma.

We note that we can obtain (A6) by requiring that Γ^i_{lk} behaves like D_k. Thus, it is not necessary that g_{ij} has an inverse to obtain (A6).

The Aesthetic Fields Program involves an infinite number of equations as Γ^i_{jk} determines the change of all tensors regardless of rank, in the manner shown previously in the appendix. However, we need only focus on Equation (A9) as this gives the change of Γ^i_{jk} itself. It is this equation that is studied in the text. Further discussion can be found in the References cited previously. We have found that (A9) has a remarkable content. We have found multiparticle solutions, in the form of lattice solutions, as well as more complex systems. We have found soliton particles characterized by the maximum (minimum) not changing in time. Also, we have found closed string particles.

An important ingredient in our work is that in integrating (A9) from the origin there is no reason for integration to be independent of path. Such a system is called nonintegrable. We have developed the theory of nonintegrable systems for equations where derivatives are given by products (as in the case with (A9)) in a series of papers which are summarized in Reference 11. In the present paper we make use of what is called the alternate or second approach to nonintegrable systems. This approach can schematically be written

(A10) $\Gamma(U) = 1/N \sum$ contribution from a neighboring point from which the field has already been determined.

The summation is over integration directions and N is the number of integration directions. This is the same integration scheme made use of in the "Arrow of Time" paper[9] where (A10) is discussed in greater detail.

REFERENCES

1. MURASKIN, M., Alternative Approach to No Integrability Field Theory, Mathematical and Computer Modelling 12 (1989), 721.
2. MURASKIN, M., Trajectories of Lattice Particles Using the New Approach to No Integrability, Mathematical and Computer Modelling 12 (1989), 1545.
3. MURASKIN, M., Three Dimensional Particle Structure Using the New Approach to Nonintegrable Aesthetic Field Theory, Preprint.
4. MURASKIN, M., Particle Behavior in Aesthetic Field Theory, International Journal of Theoretical Physics, 13 (1975), 303.
5. MURASKIN, M., Sinusoidal Solutions to the Aesthetic Field Equations, Foundations of Physics 10 (1980), 237.
6. MURASKIN, M., Nonintegrable Aesthetic Field Theory, Mathematical and Computer Modelling, 10 (1988), 571.
7. MURASKIN, M., Aesthetic Fields: A Lattice of Particles, Hadronic Journal, 7 (1984), 296.
8. MURASKIN, M., Use of Commutation Relations in No Integrability Field Theory, Applied Mathematics and Computation, 29 (1989), 271.
9. MURASKIN, M., Arrow of Time, Physics Essays 3 (1990), 448.
10. MURASKIN, M., Proceedings of the Eighth International Conference on Mathematical and Computer Modelling, April 1-4, 1991, at College Park, Maryland. To be Published.
11. MURASKIN, M., Nonintegrable Systems, Mathematical and Computer Modelling 14 (1990), 64.